Aeroacoustics Conferences
June 4-7, 2024, Rome, Italy
30th AIAA/CEAS Aeroacoustics Conference (2024)

10.2514/6.2024-3033

Aeroacoustical Analyses from the Space Launch System Artemis-I Mission

Makayle S. Kellison[1]
Department of Physics, Rollins College, Winter Park, FL, 32789, USA

Kent L. Gee[2]
Department of Physics and Astronomy, Brigham Young University, Provo, UT, 84602, USA

Whitney L. Coyle[3]
Department of Physics, Rollins College, Winter Park, FL, 32789, USA

Mark C. Anderson[4], Logan T. Mathews[5], and Grant W. Hart[6]
Department of Physics and Astronomy, Brigham Young University, Provo, UT, 84602, USA

As the frequency of rocket launches increases, accurately predicting their noise is necessary to assess structural, environmental, and societal impacts. NASA's Space Launch System (SLS) is a challenging vehicle to model because it has both solid-fuel rocket boosters and liquid-fueled engines that contribute to its thrust at launch. This paper discusses measured aeroacoustic properties of this super heavy-lift rocket in the context of supersonic jet theory and measurements of other rockets. Using four measured aeroacoustic properties: directivity, spectral peak frequency, maximum overall sound pressure level, and overall sound power level, an equivalent rocket based on merged plumes is created for SLS. With the constraint that the effective thrust and mass flow rates should match those of the actual vehicle, a method using weighted averages of the disparate plume parameters successfully reproduces SLS's desired aeroacoustic properties, yielding a relatively simple model for the complex vehicle.

I. Nomenclature

A	=	nozzle exit area, m^2
c_a	=	ambient sound speed, assumed to be 340 m/s
c_e	=	plume exit sound speed, m/s
c_{eff}	=	effective sound speed, m/s
D_e	=	nozzle exit diameter, m
D_{eff}	=	effective diameter, m
f	=	frequency, Hz
f_{pk}	=	spectral peak frequency, Hz
κ	=	convective velocity constant
$\dot{m}$	=	mass flow rate, kg/s
M_{co}	=	Oertel convective Mach number
M_κ	=	convective Mach number

[1] Undergraduate Student, Department of Physics, and AIAA Student Member.
[2] Professor, Department of Physics and Astronomy, and AIAA Associate Fellow.
[3] Associate Professor, Department of Physics, and AIAA Member.
[4] Graduate Student, Department of Physics and Astronomy, and AIAA Student Member.
[5] Graduate Student, Department of Physics and Astronomy, and AIAA Student Member.
[6] Associate Professor, Department of Physics and Astronomy.

n = quantity, referring specifically to either 2 SRBs or 4 RS-25s
η = acoustic efficiency
OAPWL = overall sound power level, dB re 1 pW
OASPL = overall sound pressure level, dB re 20 μPa
$\mathrm{OASPL_{max}}$ = overall sound pressure level in the maximum radiation direction, dB re 20 μPa
$\mathrm{OASPL_{free}}$ = overall sound pressure level in a free field, dB re 20 μPa
p = acoustic pressure, Pa
ϕ = azimuthal angle, °
$Q_{\max}$ = directivity index in the maximum radiation direction, dB
r = the distance between the launchpad and the stationary microphone, m
R = the distance between the base of the moving vehicle and the stationary microphone, m
ρ_e = plume density, kg/m^3
ρ_{eff} = effective plume density, kg/m^3
Sr = Strouhal number
T = Thrust, N
θ = polar angle with respect to the plume exhaust direction, °
$\theta_{\max}$ = maximum directivity angle, °
U_e = plume exit velocity, m/s
W = sound power, W
W_m = mechanical power, W

II. Introduction

Seventy-two orbital rockets were launched from Cape Canaveral and Kennedy Space Center in 2023, marking a record high over the previous year's fifty-seven launches but representing just a fraction of the 223 global orbital launches [1]. Among these launches are those from a host of new launch vehicles, including reusable boosters, complex engine configurations, and the thrust capability to take astronauts to Mars. Although SpaceX's Starship will likely overtake it as the most powerful successfully launched orbital rocket, at the forefront of these rockets is NASA's Space Launch System (SLS), which completed its maiden voyage in 2022. SLS and Starship are part of a group of larger rockets launching in the next decade and which prompt further study of community noise impacts as well as the effects rocket noise has on the vehicle, payloads, launch structures, and endangered species [2] [3] [4] [5]. The dramatic increase in launch cadence as well as the development of super heavy-lift launch vehicles necessitates further understanding of the characteristic noise produced during a rocket launch.

Many early launch and rocket noise-related studies (e.g. [6] [7] [8]) were compiled into source modeling approaches found in the seminal report referred to by its number, NASA SP-8072 [9], but until the past 10-15 years, relatively few studies improved on the SP-8072 methodologies [10] [11] [12]. Lubert et al. [13] sought to review historical work and recent understanding of rocket noise based, in part, on supersonic jet noise theory. As current research aims to characterize rocket acoustics based on high-fidelity experimental data from modern launch vehicles, acoustical measurements of the SLS Artemis-I mission were collected to support model development. The findings reported in this paper aim to build on past research from various launches, including the Delta IV Heavy [14], Atlas V [15], Saturn V [16], and Falcon 9 [17], and use similar, established methods for far-field rocket noise data analysis.

Measuring and analyzing the sound produced by launch vehicles at a variety of distances allows for a complete study of aeroacoustic source phenomena and subsequent propagation effects. Although measurements cannot be taken directly at the source during a launch without extraordinary difficulty, many fundamental source characteristics can be studied using far-field acoustic data. McInerny et al. [11] [18] [19] [20] [21] identified four rocket noise characteristics that support source analyses and allow for rocket and supersonic jet acoustics to be studied in conjunction: directivity, overall sound power level (OAPWL), overall sound pressure level (OASPL), and spectral peak frequency. This paper's purpose is to study SLS's aeroacoustic characteristics using far-field acoustic data collected during NASA's Artemis-I mission.

Determining each of these aeroacoustic characteristics for SLS is complicated by the disparate velocities, fuels, and sizes of its multinozzle configuration, comprised of two solid boosters and four liquid engines. In the past, rockets with multiple engines of the same type have been simplified by modeling them as an effective rocket with one equivalent engine [9]. Other, more complex approaches have been considered, involving zones with separate and merged plumes [22] [23]. However, creating an equivalent vehicle based on a nozzle with effectively equal parameters allows for aeroacoustic characteristics and scalings to be simply applied. As part of studying McInerny's [11] aeroacoustic characteristics for SLS, this paper examines multiple definitions of an equivalent rocket. Equivalence

takes two forms. First, an acoustically equivalent rocket should match SLS's measured sound power, directivity, maximum sound pressure level, and peak frequency. Second, a mechanically equivalent rocket should match SLS's thrust, mass flow rate, and mechanical power.

This paper proceeds as follows. The acoustic measurement campaign of the Artemis-I launch is first discussed, followed by several notable results from these measurements. Then, each of the aeroacoustic characteristics is defined in detail with an accompanying overview of expected values for these metrics. Finally, two possible effective rockets are compared against target values for SLS, obtained from literature and measurements, to determine their acoustic and mechanical equivalence to the original vehicle.

III. Launch & Measurement Description

During the Artemis-I mission, SLS's 39.1 MN (8.8 million lbs) of liftoff thrust made it the most powerful rocket to successfully reach orbit. The vehicle's core stage, powered by four Aerojet Rocketdyne RS-25 liquid hydrogen-oxygen engines, is flanked by two Northrop Grumman five-segment solid-fuel rocket boosters (SRBs). RS-25 startup occurred at T-4.5 s, providing $T_{\%} \approx 19\%$ of the total liftoff thrust. At T-0 s, the SRBs ignited to yield $T_{\%} \approx 81\%$ of the total thrust and should, therefore, dominate the rocket's noise radiation. Liftoff, including a vapor cloud made visible by the rarefaction portion of the SRB overpressure, is shown in Figure 1a. A closer view of the six rocket nozzles that propel SLS are shown in Figure 1b. The nozzle and other relevant parameters for each grouping of engines or boosters used in this work, obtained from a variety of published sources, are shown in Table 1. Exit velocity was derived from sea level specific impulse [24] [25], while density was inferred from thrust and other known parameters. The exit sound speed, c_e, for the SLS solid boosters is not published, but prior work [26] has used 780 m/s for the Shuttle booster, based on a value in Ref. [11]. The same reference provided plume parameters for the Shuttle version of the RS-25, with $c_e = 860$ m/s.

Table 1. Nozzle, plume, and other parameters for SLS's engines and boosters.

	NGC SLS Booster (RSRMV)	Aerojet RocketDyne RS-25
n (quantity)	2	4
T (MN)	16.0 [27]	1.86 [28]
$T_{\%}$	40.6	4.71
W_m (GW)	19.2	3.34
$W_{m,\%}$	37.1	6.45
U_e (m/s)	2400	3590
D_e (m)	3.80 [29]	2.29 [30]
ρ_e (kg/m^3)	0.245	0.035
c_e (m/s)	780	860 [11]
c_a (m/s)	340	340
A (m^2)	11.3	4.12
$A_{\%}$	29.0	10.5

The parameters in Table 1 represent our best effort to obtain physically consistent parameters from publicly available sources. However, like c_e for the boosters, there is uncertainty in other parameters, including vehicle thrust during launch. Different documents and websites list SLS liftoff thrust as anywhere from 37.0 to 39.1 MN (8.27 to 8.8 million lbs), whereas maximum published thrust of the individual boosters/engines [27] suggest as high as 41.2

MN for the vehicle. Given that the solid boosters begin to approach maximum thrust at only T+8 s, we have opted to use published maximum thrust [27] for the boosters. On the other hand, use of the published launch thrust for the RS-25s [28] in Table 1 yields almost exactly the 39.1 MN (8.8 million lbs thrust) that seems most commonly reported for the launch thrust of the vehicle and which has been used in prior analyses [31] [32]. Despite the uncertainty in the different parameters, a limited sensitivity analysis has revealed that the primary conclusions of the paper are not materially impacted by reasonable parameter variation.

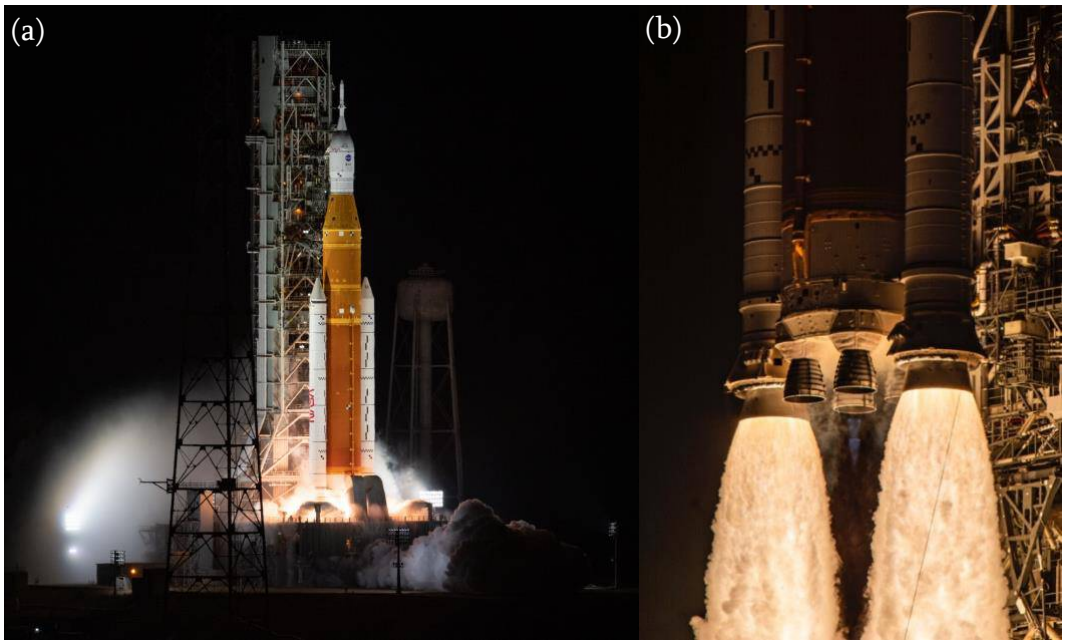

Figure 1. The Artemis-I launch: (a) SLS ignition overpressure event (visible cloud at bottom left) during liftoff. Photo credit: NASA. (b) A more detailed view of the two SRBs (larger diameter, outside) and four RS-25 engines (smaller diameter, inside). Photo credit: United Launch Alliance, used with permission.

Critical to this paper's analyses is the idea of plume merging and determining the noise generation region. As discussed by Lubert et al. [13] and partially based on vector intensity characterization of a solid rocket booster [33], the dominant noise source region spans 10 – 30 exit diameters, D_e, with a maximum source origin of around 18 D_e below the nozzle exit. Figure 2 shows the location of the 18-D_e point for both types of nozzles, indicating the SRB plumes have clearly merged into one equivalent plume. Therefore, for the purposes of comparison to jet-related scaling parameters, it is assumed that we can redefine SLS's nozzles to create an acoustically equivalent rocket comprised of a single nozzle.

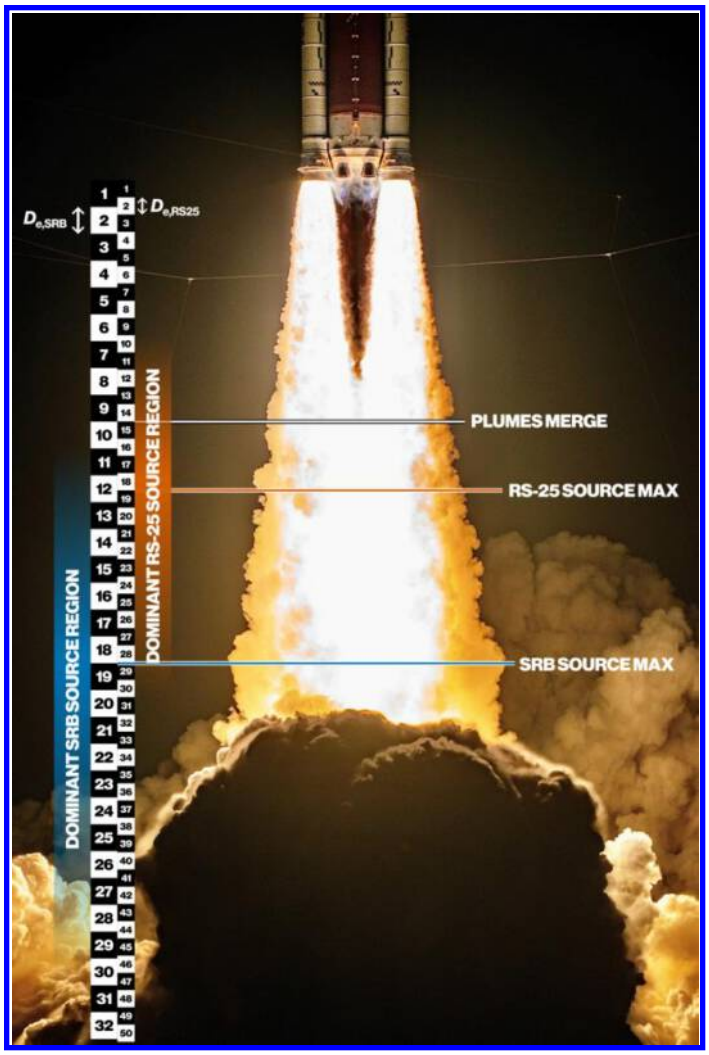

Figure 2. SLS's visible plume after the nozzle exit, with a marker indicating the beginning of the plume merging region. The rulers on the left indicate distance relative to the exit diameters of a single RS-25 and SRB, allowing for visualization of the dominant noise source region from 10-30 D_e downstream. Photograph by Josh Dinner from Space.com, used with permission.

For the Artemis-I launch, a total of fourteen acoustical measurement stations were configured. While initial analyses have been made for several of the stations [31] [34], this paper presents analyses for a subset of four stations located ~1.4 – 1.8 km from LC-39B. These stations, labeled P05, P06, P07, and P09, and their corresponding distances from the pad are shown in Figure 3. Within road access constraints, the measurement stations were strategically placed in rough cardinal directions around LC-39B to capture any azimuthal (ϕ) source directionality. These stations were the subject of an initial sound power analysis performed by Kellison and Gee [32], who discussed the lack of azimuthal asymmetry in the overall noise radiation.

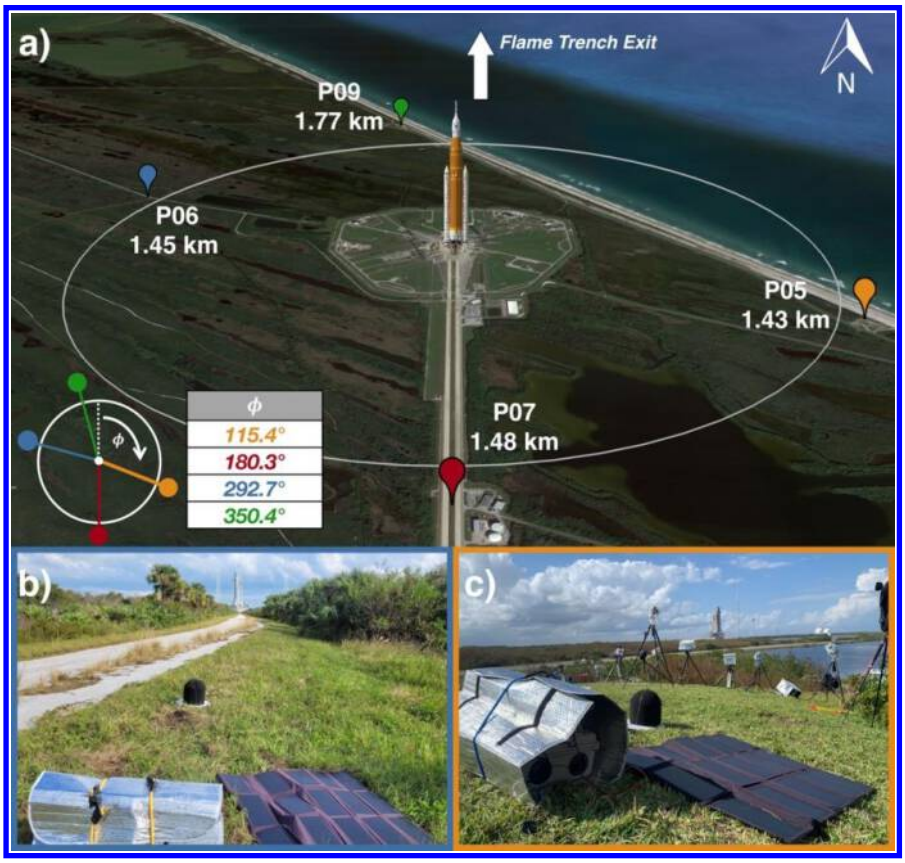

Figure 3. (a) Four autonomous measurement stations on-Center annotated with their distances and azimuths (ϕ) from LC-39B. A white circle represents the blast danger area, and a SLS model (not to scale) is included. Measurement stations P06 (b) and P05 (c) are pictured relative to the launchpad [32].

Each measurement station [35] was comprised of a ruggedized computer, GPS time clock, and 24-bit NI 9250 and 9232 data acquisition modules sampling at 102.4 kHz. At these stations, GRAS 46BE 6.35 mm (1/4 in) free-field microphones (4 Hz – 80 kHz) were used [36]. Although free-field microphones are designed for normal incidence, the response difference for other angles is insignificant at the maximum analysis frequency of 10 kHz. However, because rocket noise often includes significant energy below 4 Hz, the microphones' low-frequency responses were adjusted using digital pole-shift filtering to extend below 1 Hz [37] [38]. The microphones were set up inverted above a plastic 40.6 cm (16 in) diameter ground plate under a foam windscreen with a 3.8 cm (1.5 in) thickness. This configuration [39] is seen at station P06 in Figure 3b and at P05 in Figure 3c.

IV. Measurement Results

This analysis summarizes far-field acoustic data from four on-Center stations during SLS's launch. Findings discussed include measured waveforms and corresponding OASPL, maximum one-third-octave spectra, and an overview of OAPWL and acoustic efficiency. Some results have been reported in previous publications [31] [32] [34] but are included to provide a baseline understanding of the dataset.

A. Overall Sound Pressure Level

Observing the behavior of the measured OASPL during the early-launch, maximum-level, and late-launch periods develops both an understanding of the source and differences in level between stations over time. A pressure waveform over some time interval is transformed into OASPL (i.e., the waveform's equivalent level) as

$$\mathrm{OASPL} = 20\log_{10}\left(\frac{p_{\mathrm{rms}}}{p_{\mathrm{ref}}}\right), \tag{1}$$

where p_{rms} is the root-mean-square pressure (Pa) and p_{ref} is the reference pressure in air of 20 μPa.

Both the waveform and corresponding 1-s averaged OASPL for P05 (1.43 km) are displayed in Figure 4a. Although a single station does not provide a complete picture of the acoustic phenomena during SLS's launch, P05 was selected as representative of the data at the four stations used in this paper. The OASPLs for all four stations are plotted in Figure 4b. Although there are similarities between the curves, several notable differences emphasize the variation in measurements and are important considerations in modeling the source properties.

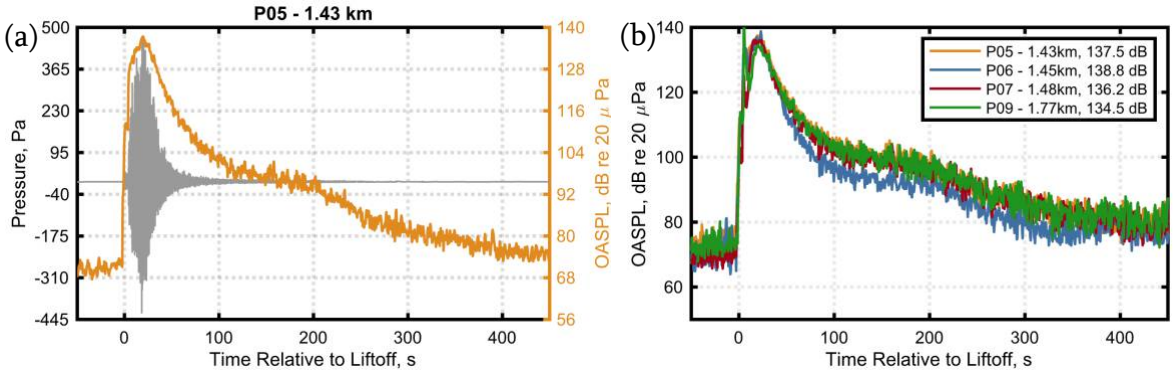

Figure 4. (a) Measured waveform (grey) and corresponding maximum OASPL (orange) for station P05, and (b) OASPLs for the four stations discussed in this paper. Maximum OASPLs and station distances are given in the legend.

First, the SRB's ignition overpressure (IOP), seen in Figure 1a, is observed in station P09's OASPL (green) in Figure 4b, where it is marked by a sharp peak around T+5 s. The maximum 1-s IOP sound level at this station was recorded as 141.2 dB, higher than the maximum level during the launch noise period. Station P07, at a similar distance located south of the pad, had lower IOP levels, with an IOP north-south variation of nearly 15 dB in peak level [31]. This can be attributed to P09's location north of the launchpad near the flame trench, indicating the directionality of the sound source during the early launch period. Second, the steep rise and fall in OASPL at all four stations reflect the relatively more rapid change in radiation angle and distance for stations closer to the source. All stations collapse relatively well around the maximum period, with an averaged $\mathrm{OASPL}_{\mathrm{max}}$ as 137 $\pm$ ~2 dB (note that these levels have not been adjusted to a common reference distance). While significant low-frequency rocket noise is still recorded beyond the abscissa limit in Figure 4, the waveforms were trimmed at 450 s to compare to stations off-Center, which were impacted by noise contamination from surrounding crowds [34]. It is noteworthy that, about 70 s after liftoff, station P06 experiences a greater decline in level than the other stations. This difference, greatest around T+100s, is believed to be in part due to a steeper low-frequency roll-off for P06's microphone and a ~1 Hz spectral peak frequency. When the digital filtering is applied to the P06 waveform, the adjusted spectrum below 1 Hz is lower level than the other three stations, resulting in a lower OASPL. Further research is needed on methods to compensate for these low-frequency roll-off differences between 6.35 mm microphones when measuring infrasound from rockets.

B. Maximum Spectra

Figure 5 displays the OTO band spectra calculated using the waveform segment corresponding to the 3 dB-down period relative to the $\mathrm{OASPL}_{\mathrm{max}}$. Two observations are made. First, the measurements had a ~10 dB/decade high-frequency roll-off characteristic of significant shock content [40] . The second observation regards the spectral peak frequency. The OTO spectra all peaked at around 20 Hz ($\pm$1 OTO band). Consistency and smoothness in the spectral shape among all four stations provides further evidence that plume merging can be assumed for SLS. Kandula [22] showed that rockets with intermediately spaced nozzles produce two defined peak frequencies corresponding to the isolated (unmerged) zone and the mixing (merged) zone. Evidence of such a double peak is not found in any of the

acoustic data collected during the Artemis-I mission, suggesting that the dominant noise source region is located below the location where the plumes begin to merge.

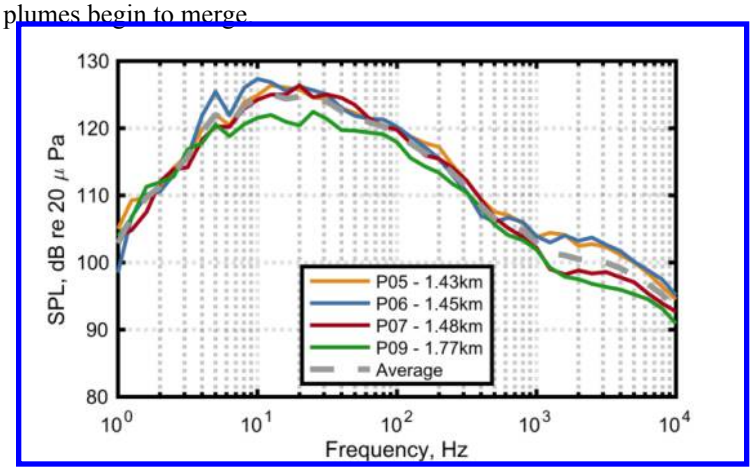

Figure 5. One-third-octave band maximum spectra from four measurement locations and their average (dashed gray).

C. Directivity & Sound Power Level

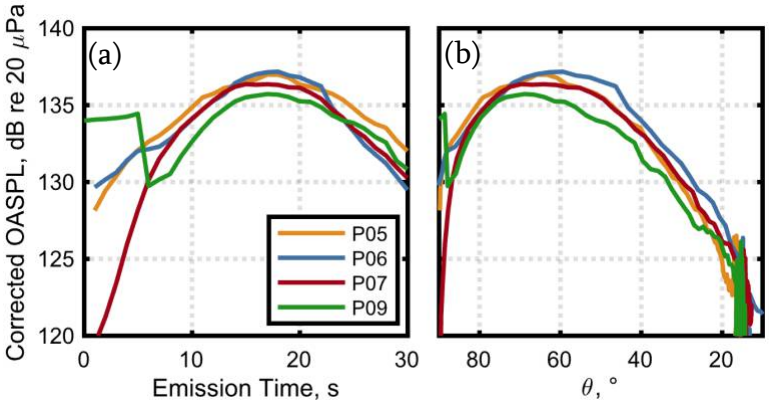

Figure 6. Artemis-I OASPLs at four measurement stations, distance-corrected to 1.43 km as a function of (a) emission time and (b) polar angle, θ.

Although a more detailed directivity discussion is reserved for the aeroacoustic analyses in Sec. V, an initial examination of the corrected OASPL(θ) in Figure 6b helps establish data validity. Across the locations, the maximum directivity angle for SLS noise radiation during liftoff ranges from 60° to 70°, with a 3 dB-down angular lobe width of around 40°. These results align with findings from other rockets. First, solid rocket boosters, including the Space Shuttle's RSRM [13] and the Atlas V's GEM-63 [41], have maximum directivity angles of 60° – 65°. Second, SLS's lobe width is consistent with the 30 – 40° lobe width observed for static firings [6] [9] [42] [43] and launched vehicles [14] [17].

Table 2 displays SLS's OAPWL for all four stations, along with their corresponding distances from LC-39B. Though representing independent measurements and calculations, all values fall within a 1 dB range, resulting in an average OAPWL of 202.4 $\pm$ 0.5 dB re 1 pW. For context, the OAPWL of an afterburning T-7A aircraft is 173 dB [44], meaning nearly 900 T-7As are required to match SLS's sound power during launch. More recent rocket noise measurements estimate the Falcon 9's OAPWL to be 196 dB [17], whereas the historic Saturn V has an estimated OAPWL of 204.7 dB [32]. Compared to other rockets, SLS's sound power is equivalent to 4.4 Falcon 9s and 0.6 Saturn Vs.

In addition to OAPWL, Table 2 also shows the calculated acoustic efficiency, η, for each station. While each vehicle's sound power differs because of nozzle size, thrust, and other plume parameters, η is used to compare OAPWL across launch vehicles and other jets. Eldred [9] compiled values for η, defined as the ratio of the vehicle's acoustic power to its mechanical power, from several studies. Most values – many from rockets much smaller than those

modern orbital launch vehicles – ranged from 0.1% to 1.0%, representing a 10 dB spread in OAPWL for a given mechanical power. Despite this data scatter, the suggestion of Mayes et al. [45] that the efficiency for rockets was about 0.5%, was adopted. Relatively recent measurements of solid-fuel rockets have reported 0.4 – 0.8% for η [13] [43] [46] [47] whereas sound power estimates from recent measurements of orbital vehicle launches have suggested values of ~0.3% [14] [17] [32]. Because significant gaps in reported calculation methodologies exist, including rigorous consideration of ground reflections [48], it is difficult to reconcile the range of reported values for η. For SLS, η ranges from 0.29 – 0.37%, with an average of 0.33%. Translated into decibels, the difference between a historically assumed 0.5% and a measured 0.33% for SLS is 1.8 dB.

Table 2. SLS's OAPWL and η presented in order of increasing distance from the launch pad.

Station	Pad Distance (km)	OAPWL (dB re 1 pW)	η (%)
P05	1.43	202.6	0.34
P06	1.45	202.9	0.37
P07	1.48	202.2	0.31
P09	1.77	201.9	0.29
Average	**1.53**	**202.4**	**0.33**

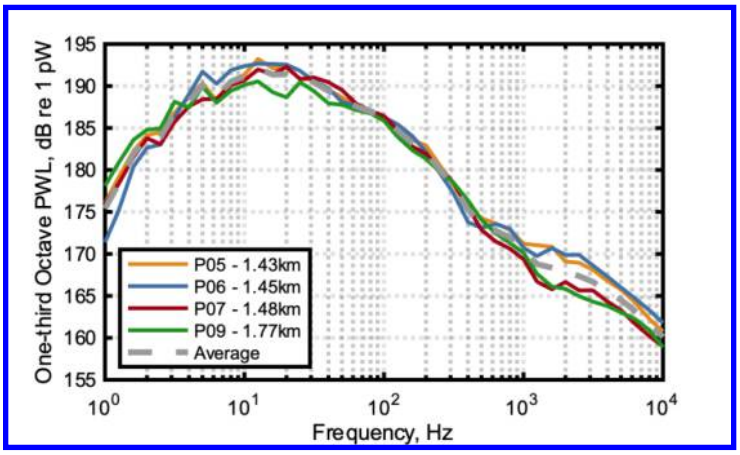

Figure 7. One-third-octave band sound power level (PWL) spectra for P05, P06, P07, and P09 located in approximate cardinal directions relative to the launchpad.

The sound power methodology used to obtain OAPWL is applied to each frequency band individually to calculate sound power level spectra, PWL(f). Figure 7 shows OTO-band PWL(f) for all four stations, with strong similarities among spectral curves. In the lowest-frequency region (< 10 Hz), the data spread across stations is ~2 – 3 dB, with relatively random scatter. Additionally, all stations have a peak frequency value of ~10 – 20 Hz with an average of approximately 17 Hz, which is similar to the maximum sound pressure level spectra in Figure 5. Between about 50 and 500 Hz, the PWL(f) from the four stations collapse remarkably well. Above 500 Hz, however, the high-frequency behavior at each station differs in a seemingly nonrandom way. The high-frequency PWL at P05 and P06 is about 5 dB greater than that at P07 and P09, but any high-frequency azimuthal asymmetry is small enough that it is ignored for the purposes of the present analysis.

V. Aeroacoustic Characteristics

Applying aeroacoustics characteristics to rocket noise data based on high-fidelity measurements contributes to the continued improvement of simple noise prediction models that scale well across rockets and jets. Improvements can be made to historical prediction methods, such as NASA SP-8072 [9], by implementing current jet noise modeling frameworks and today's understanding of fluid governing principles [13]. The most current culmination of these

revisions is outlined in this section and these metrics will be used to validate acoustic data collected during the Artemis-I launch and define an aeroacoustically equivalent vehicle.

A. Directivity

Measuring the directionality of launch vehicle noise is important in developing physics-based predictive models for noise radiation. However, there remains significant ambiguity and variation in the historical literature concerning rocket noise directivity functions. Cole et al. [6] cited the peak radiation for a launch rocket to be between 70° – 80° and in the 50° – 60° range for a horizontal static fire. For decades after Cole's 1957 [6] measurements, it was believed that maximum directivity angle, $\theta_{\max}$, differs between a launched and static fired rocket, with the latter being 10 – 20° less [11] [12] [18]. Eldred [9] reported the peak directivity angle for a standard chemical rocket to be 50°, supported by the claim that the maximum radiation angle is dependent on exhaust flow parameters (e.g., exit velocity, sound speed, density, static pressure). Similar to this work, other early reports failed to connect the noise radiation angle to the fundamental flow physics and aeroacoustic sources. Although Space Shuttle booster static measurements [42] [49] initially were thought to confirm the historical static-fire directivity pattern, other work [13] [26] [50] has shown that this pattern was distorted by the true acoustic source location being located downstream of the nozzle exit. Today it is understood that Mach wave radiation, created by supersonically convected large-scale turbulence, is the main contributor to the noise directionality (e.g. [11] [51] [52]). As such, some characteristic convective Mach number can be used to predict the directivity for a given rocket.

Greska et al. [53] defined the Oertel convective Mach number as the arithmetic mean of two other convective Mach numbers observed by Oertel [54]:

$$M_{\mathrm{co}} = \frac{U_e + \frac{1}{2}c_e}{c_e + c_a}, \tag{2}$$

where U_e is the plume exit velocity (m/s), c_e is the exit sound speed (m/s), and c_a is the ambient sound speed (assumed to be 340 m/s). The peak directivity angle can be written in terms of Oertel convective Mach number as

$$\theta_{\max} = \cos^{-1}\left(\frac{1}{M_{\mathrm{co}}}\right). \tag{3}$$

This model has been successfully used to describe the peak directivity angle for large-scale solid rocket motors [41] [26], and the parameters in Lubert et al. [13] suggest a peak directivity angle between 62° and 72° for solid and liquid fuel rockets. As an example, M_{co} for an Atlas V rocket was found to be 3.1, yielding a predicted $\theta_{\max}$ of 71.2° [15]. Equation (2) was also applied to acoustical measurements of a Falcon 9 [17], with a predicted $\theta_{\max}$ of 69° and corresponding M_{co} of 2.81. A measured $\theta_{\max}$ of 64° was reconciled with theory by accounting for the large measurement distance and a nonnegligible vehicle Mach number. On the other hand, M_{co} provided excellent agreement, within 0.5°, with the measured 70.4° averaged over several closer measurement stations and a slowly moving Delta IV Heavy [14].

There are other definitions of convective Mach number used in supersonic jet noise literature. One commonly used model defines the convective velocity as some fraction, κ, of U_e, such that the peak angle is predicted by

$$\theta_{\max} = \cos^{-1}\left(\frac{1}{M_\kappa}\right) = \cos^{-1}\left(\frac{c_a}{\kappa U_e}\right). \tag{4}$$

In Eq. (4), κ typically ranges from 0.6-0.85 in the supersonic jet literature. Mathews et al. [17] hypothesized that these values were incorrect for rockets and suggested the Falcon 9 had a κ value of 0.31. An analysis by Lubert et al. [13]

of Bassett et al. [41] GEM-63 data suggested $\kappa \approx 0.32$. Based on these works, $\kappa \approx 0.31$ is assumed hereafter in this paper.

B. Peak Frequency

Spectral peak frequency, f_{pk}, is the second aeroacoustic characteristic relevant to this discussion. This could refer to the sound pressure level spectrum at $\theta_{\max}$ or the sound power level spectrum, PWL(f). Strouhal number (Sr), defined as the ratio of some effective diameter relative to some effective velocity, has been used to scale PWL(f) across rockets and jets when exit variables (nozzle diameter, thrust, velocity, temperature) vary. Although different Strouhal definitions have been explored for rockets (see [11], [13], [17], and references therein), NASA SP-8072 includes PWL(Sr) for different rockets using the traditional definition,

$$\mathrm{Sr} = \frac{f D_e}{U_e}, \tag{5}$$

where f is the frequency (Hz), D_e is the nozzle exit diameter (m), and U_e is the plume exit velocity (m/s). Eldred [9] found $\mathrm{Sr}_{\mathrm{pk}}$ for the sound power level spectrum to be 0.020, and McInerny 1991 discussed a similar value, referencing the data from Cole et al. [6]. Several other measurements have scaled maximum sound pressure level spectra by Strouhal number, including the RSRM with a peak $\mathrm{Sr}_{\mathrm{pk}} = 0.025$ [13], the Falcon 9 with a peak $\mathrm{Sr}_{\mathrm{pk}} = 0.019$ [17], and the Atlas V with a peak $\mathrm{Sr}_{\mathrm{pk}} = 0.018$-$0.020$ [55]. However, it should be noted that sound pressure level spectra and PWL(f) are similar but not identical for a given launch vehicle and some reports involve using fractional-octave data whereas others involve narrowband or narrowband-equivalent spectra. At present, the best estimate for a PWL(Sr) is that contained in Eldred [9], with $\mathrm{Sr}_{\mathrm{pk}} = 0.020$.

C. Maximum Overall Sound Pressure Level

Connected to directivity is the OASPL in the maximum radiation direction, $\mathrm{OASPL}_{\max}$. Greska [53] proposed an empirical model for predicting maximum overall sound pressure level at 100 D_e for a broad range of jets, including rockets, based on the Oertel convective Mach number in Eq. (2). For the rockets considered, Greska [53] found the $\mathrm{OASPL}_{\max} = 143 – 144$ dB at 100 D_e. While the empirical data fit provided by Greska as a function of M_{co} is uncertain, recent work has suggested similar maximum overall levels for both static and launched rockets at the same scaled distance (100 D_e or 100 D_{eff}, as appropriate). Reported measurements for a Falcon 9 at 100 D_{eff} were 143 dB [17] and 143 – 144 dB for GEM-63 static firings [41]. The RSRM maximum level, measured by Kenny et al. [42], was calculated to be 143 dB at 80 D_{eff}, which translates to ~141 dB at 100 D_{eff}. However, James et al. [47] predicted nearly 145 dB for the RSRM at 100 D_{eff} using an SP-8072-based model with updated directivity functions. Further work is necessary to confirm the validity, but the limited results available suggest an average of ~143.5 dB at 100 D_{eff} for rockets, without a clear dependence of level on convective Mach number. This value will be assumed as a target value for the remainder of the paper.

Two models are used here to predict $\mathrm{OASPL}_{\max}$ at 100 D_{eff} from measured data. The first finds $\mathrm{OASPL}_{\max}$ using levels measured at horizontal range, r, from the launchpad, and applying spherical spreading:

$$\mathrm{OASPL}_{\max} = \mathrm{OASPL} + 20\log_{10}\left(\frac{r}{100 D_{\mathrm{eff}} \sin(\theta_{\max})}\right). \tag{6}$$

McInerny [11] [18] also developed a relatively simple model that relates OAPWL to $\mathrm{OASPL}_{\max}$. One caveat, however, has been the explicit accounting for ground reflections in McInerny's original model, which may have altered $\mathrm{OASPL}_{\max}$ estimates. The version of the McInerny model presented in this paper builds on recent work [48] [55] that alters the original formula. Based on a measured OAPWL, McInerny's model then determines the maximum level in a free field environment, $\mathrm{OASPL}_{\mathrm{free}}$, through

$$\mathrm{OASPL}_{\mathrm{free}} = \mathrm{OAPWL} - 10\log_{10}(4\pi R^2) + Q_{\max}, \tag{7}$$

where R is the distance between the base of the moving vehicle and the stationary microphone. For the purposes described here, we set $R = 100D_{\mathrm{eff}}$. $Q_{\max}$ represents the directivity index in the maximum radiation direction. Historically, $Q_{\max}$ has been assumed to be 8 dB, based on analyses by Cole et al. [6]. However, Mathews et al. [55] have found that for free-field definitions of OAPWL and OASPL, 3 dB must be subtracted from $Q_{\max}$. Therefore, $Q_{\max} \approx 5$ dB.

A recent study [48] of rocket noise incident on finite-impedance ground surfaces has shown that pressure doubling (+ 6 dB) can be assumed for microphones at the ground, except where the ground is especially porous. Implementing McInerny's model provides an additional method for comparing $\mathrm{OASPL}_{\max}$ against the predicted ~143.5 dB at 100 D_{eff}. Because $\mathrm{OASPL}_{\mathrm{free}}$ assumes free-field conditions, $\mathrm{OASPL}_{\max}$ is written from Eq. (7) as

$$\mathrm{OASPL}_{\max} = \mathrm{OASPL}_{\mathrm{free}} + 6, \tag{8}$$

where + 6 represents the 6 dB level increase due to pressure doubling.

D. Overall Sound Power

From directivity information, a rocket's radiated sound power, OAPWL, can be calculated using far-field acoustic data. However, a rocket's sound power can also be calculated directly from the plume mechanical power. Using known values for the mechanical power of a rocket, W_m, and an assumed efficiency, η,

$$\mathrm{OAPWL} = 10\log_{10}\left(\frac{\eta W_m}{W_{\mathrm{ref}}}\right), \tag{9}$$

where W_{ref} = 1 pW. In Section IV.C, the average η was found to be 0.33% for SLS [32], the value that is used for the remainder of this paper. The mechanical power model provides methods of estimating OAPWL that can be compared to the calculated sound power level in Table 2 for further evaluation of an equivalent vehicle.

VI. Analysis

The measured acoustical characteristics and their relationship to plume and vehicle parameters may be used to create an SLS-equivalent rocket, both mechanically and acoustically. An equivalent vehicle reduces the complexity of SLS's nozzle configuration with multiple solid boosters and liquid engines. Such an effective vehicle will have only one circular nozzle that combines the parameters of both the two SRBs and the four RS-25s. Due to the differences in fuel type, flow parameters, size, and quantity of SLS's engines and motors, care must be taken to create appropriate effective parameters. This section discusses two approaches to creating effective launch vehicles for SLS. The first approach describes a rocket comprised of only the two SRBs and the second approach accounts for both SRBs and the four RS-25s using weighted averages. Each approach is accompanied by corresponding methodology and an evaluation using the previously described aeroacoustic characteristics to determine the vehicle's equivalence to SLS.

A. Effective Rocket 1: SRBs Only

During the Artemis-I launch, the SRB's provided more than 80% of SLS's thrust and ~75% of the vehicle's power, suggesting they dominate the overall noise radiation. Given this contribution, the first effective rocket to be evaluated is based on the metrics of an SLS vehicle with only SRB motors. The equivalence of this SRB-only vehicle to target values from SLS measurements or the literature helps to assess the relative contributions of the SRBs to the total radiated noise.

Both effective rockets are assigned specific values for the following four exit parameters: effective diameter, velocity, density, and sound speed. For the first effective rocket comprised of two SRBs, most parameters are listed in Table 1 and are equivalent to those of a single SLS SRB. The effective diameter was found using the traditional merged-plume formula [9] where $D_{\text{eff}} = \sqrt{2}D_{\text{e,SRB}}$, corresponding to the number of boosters and resulting in D_{eff} = 5.37 m. With these effective parameters, the rocket comprised of two merged SRBs is evaluated based on five major checks, resulting in seven metrics, to compare its acoustical and mechanical characteristics to those of the actual SLS rocket.

The aeroacoustic checks for the two-SRB rocket are summarized in Table 3 and displayed alongside the target SLS values as well as the relative error between them. Each of the checks are discussed briefly following these results.

Table 3. Aeroacoustic metrics applied to the first effective rocket, comprised of two SRBs.

	Units	2 SRBs	Target Value	Target Source	|Error|
T	MN	32.0	39.1	Published	18.1%
$\theta_{\max}(M_{\text{co}})$ (Eq. 3)	degrees	66.3	65.7	Measured	0.6°
$\theta_{\max}(M_{\kappa})$ (Eq. 4)	degrees	62.8	65.7	Measured	2.9°
Sr_{pk} (Eq. 5)	---	0.012	0.02	Literature	2.4 OTO Bands
$\text{OASPL}_{\max}$ (Eq. 6)	dB re 20 μPa	147.0	143.5	Literature	3.5 dB
$\text{OASPL}_{\max}$ (Eq. 8)	dB re 20 μPa	147.8	143.5	Literature	4.3 dB
OAPWL (Eq. 9)	dB re 1 pW	201.0	202.4	Measured	1.4 dB

1. Thrust

Summing the thrust of two SRBs (see Table 1) produces a combined liftoff T = 32.0 MN for the first effective rocket, about 81% of the actual vehicle's thrust. Although expected, this first effective vehicle falls ~18% short of having equal thrust as SLS, based on the known contributions of the RS-25 main engines to the total T.

2. Convective Mach Number

The definitions of convective Mach number in Eqs. (3) and (4) are used to determine if this effective rocket radiates sound at the same angle as SLS. Averaging the four directivity curves in Figure 6b results in Figure 8, which has a peak directivity angle, $\theta_{\max}$, of 65.7°. This represents the target value for convective Mach number-based comparisons, although the shaded region indicates some uncertainty in this estimate.

Using Eq. (3), M_{co} predicts $\theta_{\max}$ = 66.3° for an effective rocket comprised of 2 SRBs. This overestimates SLS's measured directivity angle by 0.6°, but falls within the expected range based on the shaded region representing the min/max bounds in Figure 8 and other predictions made using this model. For example, M_{co} predicts the Falcon 9 directivity angle within 5° [17] and the Delta IV Heavy within <1°[14]. Equation (4) predicts $\theta_{\max}$ = 62.8°, about 2.9° less than SLS's value but still seems within the bounds of reasonable uncertainty. Thus, for the SRB-only vehicle, the $\theta_{\max}$ predictions made using M_{co} and M_{κ}, match SLS's directivity with a relatively small error. Therefore, it can be concluded that an effective rocket comprised of only SRBs would radiate its maximum noise approximately in the same direction as SLS. Because the RS-25 engines by themselves have a predicted $\theta_{\max}$ > 72° using either definition of convective Mach number, this result confirms the prior assumption that the SRBs dominate the overall noise radiation of the vehicle.

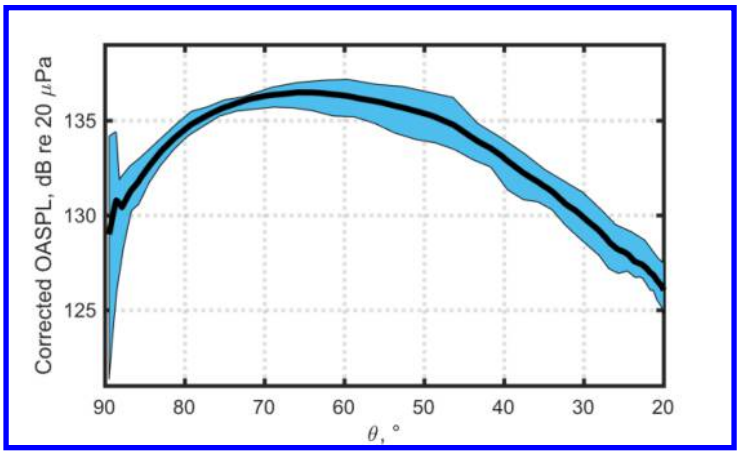

Figure 8. Distance-corrected OASPL, averaged between P05, P06, P07, and P09, as a function of polar angle, θ (black line). Bounds from the maximum and minimum values at each angle are indicated by blue shading.

3. Strouhal Number

With this effective rocket matching SLS's directivity but differing appreciably in thrust, the next check of D_{eff} = 5.37 m is by examining the Strouhal-scaled sound power level spectrum, PWL(Sr). The average PWL(f) from Figure 8 was scaled by the Sr definition in Eq. (5). The normalized PWL(Sr) for the SRB effective rocket is shown in conjunction with the sound power spectrum from NASA SP-8072 [9]. Relative to the SP-8072 curve, the "SRB-only" rocket has a PWL(Sr) that appears shifted well to the left, with a peak at Sr = 0.012 that is obtained using a second-order polynomial curve fit. With an error of 2.40 OTO bands between Sr = 0.012 and Sr = 0.020 – nearly one octave – this effective vehicle is much lower in frequency than Eldred's model [9]. The results suggest that the effective diameter, $\sqrt{2}D_{\text{e,SRB}}$, could be too small or that $U_{\text{eff}} = U_{\text{e,SRB}}$ is too large. This latter scenario is much less likely, as the actual U_{eff} accounting for both the SRBs and the RS-25s is likely to be greater than $U_{\text{e,SRB}}$ given that the exit velocity of the RS-25 is significantly greater than that of the SRBs (Table 1). Either the historical PWL curve does not hold for SLS or D_{eff} is too small.

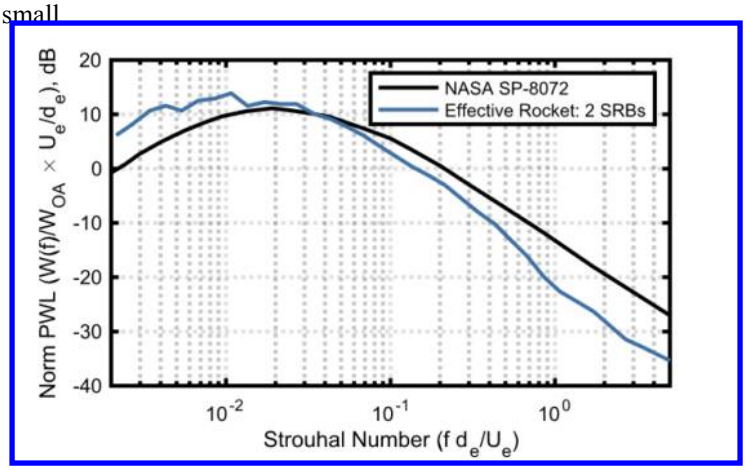

Figure 9. Normalized average sound power spectrum for SLS scaled by Sr using the effective parameters from a 2 SRB-rocket (blue) and plotted against a historical spectrum (black) for comparison [9].

4. Maximum Overall Level

Checking the $\text{OASPL}_{\text{max}}$ of each effective vehicle ensures that it matches the propagation behavior of other measured rockets at the same scaled distance. This is a further check of the D_{eff} definition. Employing spherical spreading in Eq. (6) results in a maximum OASPL of 147.0 dB at 100 D_{eff}. This is 3.5 dB greater than the target value of 143.5 dB, discussed in Sec. V.C. If instead Eq. (8) is applied with this D_{eff}, a decision has to be made regarding which OAPWL value to use. Because there is not an independent OAPWL measurement of an SRB-only rocket, the OAPWL must be estimated. Using the calculated level from the section below results in an $\text{OASPL}_{\text{max}}$ of 146.4 dB.

This effective vehicle, with only 81% of SLS's thrust, predicts a maximum OASPL approximately 3 dB greater than the assumed value of 143.5 dB with this D_{eff} definition. Either SLS noise radiation does not follow the trend on which the target value is based, or it strengthens the argument that D_{eff} is too small. A difference of ~3 dB in level suggests D_{eff} needs to be at least 50% larger than the SRB-only version to match the target value.

5. Overall Sound Power

The final check to ensure this theoretical rocket's acoustical and mechanical equivalence to SLS is related to the vehicle's radiated sound power, OAPWL. Using the known mechanical power of the effective rocket, which is the sum of the mechanical power of two SRB motors, the OAPWL can be calculated following Eq. (9) and assuming $\eta = 0.33\%$. The predicted OAPWL of the effective rocket is 201.0 dB, with only a 1.4 dB error. Similar to the effective vehicle's reduced thrust, only accounting for a portion of the mechanical power (75%) results in an underprediction of the OAPWL. Conversely, this analysis indicates that the combined effect of four RS-25s is to add a little more than 1 dB to SLS's OAPWL of 202.4 dB.

B. Effective Rocket 2: SRBs and RS-25s

Some of the aeroacoustics metrics, such as directivity angle and OAPWL, for the first effective rocket containing two SRBs matched the actual vehicle relatively well, with low errors shown in Table 3. However, this vehicle was not mechanically equivalent to SLS, with 19% less thrust and 25% less mechanical power due to the absence of the RS-25s, and metrics such as D_{eff}-scaled $\text{OASPL}_{\text{max}}$ and Sr_{pk} were relatively far from target values. Despite the SRBs dominating the noise radiation of SLS, the RS-25 engines must be incorporated into the effective vehicle to develop an aeroacoustically equivalent rocket. The comparison between the SRB-only and full equivalent vehicles also provides a baseline to further understand the impact of the RS-25 engines on the overall noise radiation.

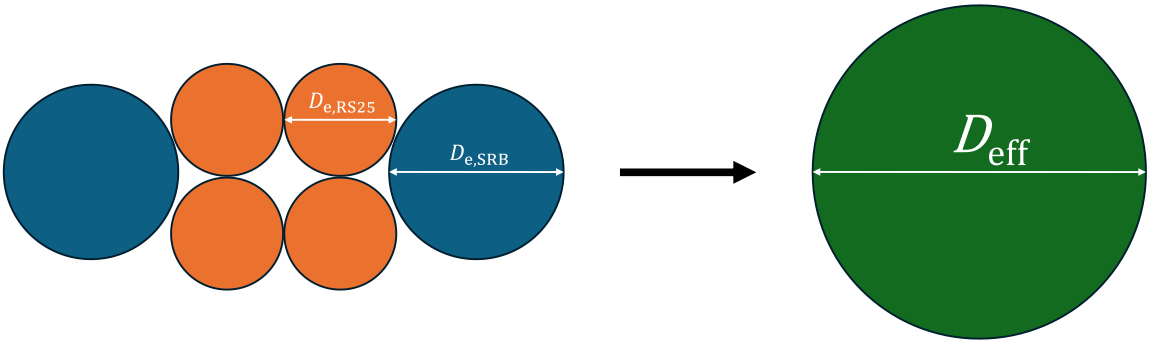

Figure 10. The nozzle configuration of SLS's SRBs and RS-25 engines is shown (left), labeled with their individual diameters, alongside the single nozzle of SLS_{eff} (right), with its effective diameter. The comparative geometries are to scale.

The second equivalent rocket, SLS_{eff}, has effective parameters that incorporate metrics from both the solid boosters and liquid engines, essential creating a rocket where SLS's disparate plumes instantly merged. Figure 10 shows a schematic involving a to-scale bird's eye view of SLS's multinozzle configuration, and the singular nozzle of SLS_{eff} with D_{eff} calculated as,

$$D_{\text{eff}} = \sqrt{2D_{\text{e,SRB}}^2 + 4D_{\text{e,RS25}}^2}, \tag{10}$$

where $D_{\text{e,SRB}}$ is the diameter of one SRB (see Table 1) and $D_{\text{e,RS25}}$ is the diameter of one RS-25 (see Table 1). As shown in Table 4, the resulting $D_{\text{eff}} = 7.06$ m. It is of note that this diameter is ~31% larger than the SRB-only rocket, suggesting at least partial reconciliation of the $\text{OASPL}_{\text{max}}$ differences discussed in Sec. VI.A.4.

Beyond diameter, effective parameters were also calculated for exit velocity, density, and sound speed using a combination of the RS-25 and SRB metrics. To find the effective density of the fluid flow at the nozzle, ρ_{eff}, the plume was modeled using its cross-sectional area, A. The average density of the plume's cross-section was found by

weighting the SRB and RS-25 plume densities by their respective area contributions. The percentage area of each engine type was found using

$$A_{\%} = \frac{nA}{2A_{\mathrm{SRB}} + 4A_{\mathrm{RS25}}}, \tag{11}$$

where n is the number of engines (two or four) and A is the area of one SRB or RS-25. Using these percentages as well as the individual exit densities, ρ_e, displayed in Table 1 $\rho_{\mathrm{eff}} = 0.157$ kg/m^3 from

$$\rho_{\mathrm{eff}} = A_{\%,\mathrm{SRB}}\rho_{\mathrm{e,SRB}} + A_{\%,\mathrm{RS25}}\rho_{\mathrm{e,RS25}}, \tag{12}$$

where $A_{\%,\mathrm{SRB}} = 58.0\%$ representing the percent area occupied by two SRBs, $\rho_{\mathrm{e,SRB}}$ is the exit density of a SRB (Table 1), $A_{\%,\mathrm{RS25}} = 42.0\%$ representing the percent area occupied by four RS-25 engines, and $\rho_{\mathrm{e,RS25}}$ is the exit density of a RS-25 (Table 1).

The second effective parameter to be calculated is the rocket's effective sound speed, c_{eff}. Table 1 gives the values for the individual sound speeds of the SRBs and RS-25 engines, which range from 780 m/s to 860 m/s. Given this range, it is reasonable to find an effective sound speed using a similar area-weighted method. The c_{eff} was found to be 814 m/s from

$$c_{\mathrm{eff}} = A_{\%,\mathrm{SRB}}c_{\mathrm{e,SRB}} + A_{\%,\mathrm{RS25}}c_{\mathrm{e,RS25}}, \tag{13}$$

Where $c_{\mathrm{e,SRB}}$ is the sound speed of one SRB (Table 1) and $c_{\mathrm{e,RS25}}$ is the sound speed of one RS-25 (Table 1). Note that c_{eff} is only used in the calculation of M_{co}, used to find θ_{max} in Eq. (3). The range of possible values for c_{eff} from 780 m/s to 860 m/s was found to only change θ_{max} by 2 – 3°, providing further justification for the reasonableness of the area-weighting method.

For effective velocity, U_{eff}, weighting by A does not accurately encompass the respective contributions of the SRBs and the RS-25's to the rocket's thrust. Therefore, instead of area-weighting U_e directly, mass flow rate, $\dot{m}$, is instead area-weighted and used to calculate U_{eff}. As $\dot{m}$ is given by

$$\dot{m} = \rho_e A U_e, \tag{14}$$

the known parameters of exit density, ρ_e, and area, A, can be used in calculating U_{eff}. The mass flow rate of SLS$_{\mathrm{eff}}$ is calculated as follows:

$$\rho_{\mathrm{eff}}A_{\mathrm{eff}}U_{\mathrm{eff}} = \rho_{\mathrm{e,SRB}}A_{\mathrm{SRB}}U_{\mathrm{e,SRB}} + \rho_{\mathrm{e,RS25}}A_{\mathrm{RS25}}U_{\mathrm{e,RS25}}, \tag{15}$$

where $A_{\mathrm{eff}} = 39.1$ m^2 represents the total area of the effective rocket's cross-sectional plume. From this equation, U_{eff} can be found as,

$$U_{\mathrm{eff}} = \frac{\rho_{\mathrm{e,SRB}}A_{\%,\mathrm{SRB}}U_{\mathrm{e,SRB}} + \rho_{\mathrm{e,RS25}}A_{\%,\mathrm{RS25}}U_{\mathrm{e,RS25}}}{\rho_{\mathrm{eff}}}, \tag{16}$$

where the SRB and RS-25 areas have been replaced by their respective percentages. U_{eff} of this rocket was found to be 2510 m/s. Summarized in Table 4, these SLS$_{\mathrm{eff}}$ parameters can be applied to determine the mechanical and acoustical equivalence of this vehicle to SLS.

Table 4. Nozzle parameters for an effective rocket that incorporates two SRBs and four RS-24 engines.

	Effective Parameters
U_{eff} (m/s)	2510
D_{eff} (m)	7.06
ρ_{eff} (kg/m^3)	0.157
c_{eff} (m/s)	814

The seven metrics from the five aeroacoustic checks are shown in Table 5 in addition to their target values and the error between them. Evaluation of each metric determines if $\mathrm{SLS}_{\mathrm{eff}}$ is a more meaningful effective rocket than one comprised of only two SRBs, and also determine the relative contribution of the RS-25 engines in the effective parameters used to calculate aeroacoustic metrics.

Table 5. Aeroacoustic metrics applied to the second effective rocket, comprised of parameters from two SRBs and four RS-25 engines.

	Units	$\mathrm{SLS}_{\mathrm{eff}}$	Target Value	Target Source	|Error|
T	MN	38.7	39.1	Published	1.0%
$\theta_{\max}(M_{\mathrm{co}})$ (Eq. 3)	degrees	66.7	65.7	Measured	1.0°
$\theta_{\max}(M_{\kappa})$ (Eq. 4)	degrees	64.1	65.7	Measured	1.6°
$\mathrm{Sr}_{\mathrm{pk}}$ (Eq. 5)	---	0.015	0.020	Literature	1.3 OTO Bands
$\mathrm{OASPL}_{\max}$ (Eq. 6)	dB re 20 μPa	144.7	143.5	Literature	1.2 dB
$\mathrm{OASPL}_{\max}$ (Eq. 8)	dB re 20 μPa	145.4	143.5	Literature	1.9 dB
OAPWL (Eq. 9)	dB re 1 pW	202.1	202.4	Measured	0.3 dB

1. Thrust

Calculating the thrust, T, of $\mathrm{SLS}_{\mathrm{eff}}$ determines the mechanical equivalence of this rocket to SLS. Using

$$T = \frac{\pi}{4}\rho_{\mathrm{eff}} D_{\mathrm{eff}}^2 U_{\mathrm{eff}}^2 \tag{17}$$

yields T = 38.7 MN for $\mathrm{SLS}_{\mathrm{eff}}$, only 1.0% lower than the 39.1 MN that the actual rocket produces. This result confirms the reasonableness of the effective variables obtained by incorporating the RS-25s into each parameter.

2. Convective Mach Number

The second check determines if $\mathrm{SLS}_{\mathrm{eff}}$ radiates noise at a similar angle to the actual vehicle using convective Mach number to predict $\theta_{\max}$. Equation (3) for M_{co} predicts a directivity angle of $\theta_{\max}$ = 66.7°, nearly identical to the effective rocket comprised of 2 SRBs. On the other hand, using M_{κ} in Eq. (4) predicts $\theta_{\max}$ = 64.1°, 1.6° less than SLS's peak directivity. This increase of $\theta_{\max}$ by a little more than 1.0° from the SRB-only vehicle is due to the increase in U_{eff}. Overall, the similarity in these results further suggests that the RS-25s do not contribute dramatically contribute to the rocket's overall peak directivity, aligning with the conclusion from the previous section. Regardless of definition or effective vehicle type, errors are less than 3°.

3. Strouhal Number

While differences in directivity between the two effective rockets are somewhat inconclusive, spectral scaling provides more clarity. Shown in Figure 11 alongside the Sr-scaled sound power spectrum from NASA SP-8072 [9], the SLS_{eff} normalized sound power level spectrum peaks at Sr = 0.015, closer to the target value of 0.02. SLS_{eff} falls short of this peak by 1.30 OTO bands, which is significantly more accurate than the previous effective vehicle that was 2.40 OTO bands less than Eldred's peak. Because of the limited use of Sr scaling in rocket noise literature, it is still inconclusive as to if Sr = 0.020 is the "ideal" peak frequency for the super heavy-lift launch vehicles of today's space industry. But the result in Figure 11 is more representative of historical rockets used to produce the SP-8072 curve.

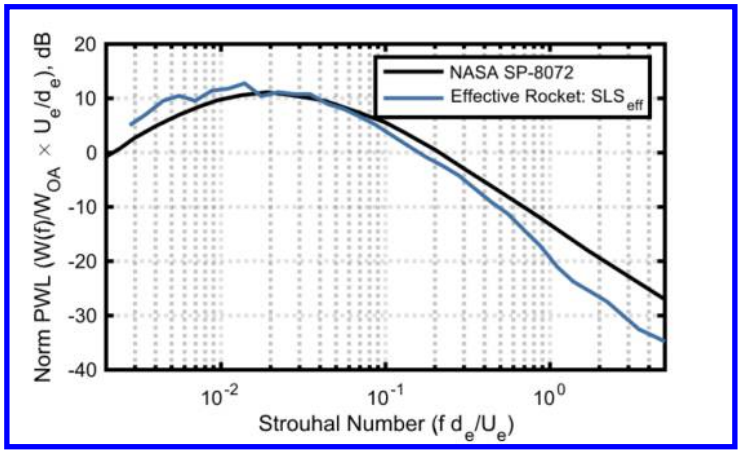

Figure 11. Normalized average sound power spectrum for SLS scaled by Sr using the effective parameters from SLS_{eff} (blue) and plotted against a historical spectrum (black) for comparison [9].

4. Maximum Overall Level

For $OASPL_{max}$, the spherical spreading-only model in Eq. (6) predicts a level of 144.7 dB at 100 D_{eff} whereas the OAPWL-based model in Eq. (8) predicts a level of 145.4 dB. These are closer to the target value of 143 – 144 dB, producing together an error of 1.6 dB when compared to 143.5 dB. Though the agreement is not perfect, the target is based on limited data and it is uncertain if spherical spreading exactly holds or if nonlinear propagation effects play a role. Likewise, these results could imply that the Q_{max} = 5 dB in the revised McInerny model needs refinement. Thus, an error of less than 2 dB in $OASPL_{max}$ seems an acceptable level of error for SLS_{eff}'s equivalence to the actual vehicle.

5. Overall Sound Power

The final aeroacoustic metric to use in comparing the effective rocket with SLS is OAPWL, which incorporates both acoustic and mechanical elements of the vehicle. From prior work [32], SLS's measured OAPWL was found as 202.4 dB. Using Eq. (9) and an assumed η = 0.33% with the effective parameters in Table 4, SLS_{eff}'s OAPWL = 202.1 dB. This near equivalence suggests that the effective parameters not only match SLS's thrust, but also the vehicle's mechanical power, which is nearly proportional to U_{eff}^3.

VII. Conclusion

This paper has provided an aeroacoustical analysis of NASA's SLS based on high fidelity data collected during the Artemis-I mission. Four aeroacoustic characteristics were examined: overall sound power level (OAPWL), peak Strouhal number (Sr_{max}) of the sound power level spectrum (PWL(f)), maximum directivity angle (θ_{max}), and maximum overall sound pressure level ($OASPL_{max}$) at 100 effective diameters (D_{eff}). Based on the assumption that all SRB and RS-25 plumes merge upstream of the dominant noise-producing region, collective evaluation of these metrics led to the development of an equivalent rocket, matching SLS's mechanical and acoustical properties. To create such an equivalent rocket, effective parameters, for diameter, velocity, sound speed, and density, were defined using the plume parameters from SLS's engines and motors.

Of importance is that the equivalent vehicle's thrust matched SLS's liftoff thrust of 39.1 MN. An effective rocket comprised of only two SRBs was first suggested based on the assumption that the SRBs dominate the overall power

and noise radiation. However, it was found that an SRB-only effective rocket fell short of matching SLS's thrust, in addition to disparities in other acoustical properties. Therefore, an equivalent rocket that integrated both the SRB and RS-25 parameters was created to match the outlined mechanical and acoustical checks. This equivalent SLS rocket, SLS_{eff}, has a thrust of 38.7 MN, only 1.0% less than the actual vehicle.

From prior work [32], SLS's OAPWL was found to be 202.4 dB re 1 pW, with a corresponding acoustic efficiency, η, of 0.33%. For SLS_{eff}, an OAPWL of 202.1 dB was calculated from the effective plume parameters, assuming η = 0.33%. A difference of 0.3 dB in OAPWL indicates near mechanical power equivalence between the effective and actual vehicles, in addition to the thrust equivalence.

A frequency-dependent approach was next used to evaluate SLS_{eff}'s exit diameter and velocity. The PWL(f) was scaled on a Sr axis, using SLS_{eff} plume parameters. The Sr_{max} of this spectrum was found to be 0.015, slightly less than the historically assumed value of Sr_{max} = 0.02. However, it is unclear as to if this historical estimate holds for modern launch vehicles, suggesting the need for additional comparisons in the future.

To further evaluate SLS_{eff}'s exit velocity along with its exit sound speed and their role in determining the directionality of the rocket's noise radiation, two definitions of convective Mach number were applied. The average θ_{max} = 65.4°, less than 0.5° from SLS's measured value. This difference is likely within the measurement uncertainty. Notably, the SRB only effective vehicle produced an average θ_{max} = 64.6°, suggesting that the peak radiation angle is dominated by the SRB conditions.

The final characteristic, $OASPL_{max}$, was calculated to further check SLS_{eff}'s exit diameter and determine any patterns in distance-scaled levels. Two models were used to find SLS_{eff}'s $OASPL_{max}$ at 100 D_{eff}, and the average of these values is 145.1 dB re 20 μPa. Although values range from 141-145 dB in the literature, a target value of $OASPL_{max}$ = 143.5 dB was assumed for comparison purposes. The difference, based on measured results 1.4 -1.8 km from the pad, is 1.6 dB. This variation, however, does prompt further work in evaluating if there is a common level dependence at a scaled nozzle diameter distance. The current data are too limited to make any definite conclusions. Therefore, SLS_{eff}'s $OASPL_{max}$ matches approximately what is expected for rockets.

The results from this aeroacoustic analysis indicate that rockets with complex engine/booster/nozzle configurations can be approximated with one equivalent plume to create a reasonable aeroacoustically and mechanically equivalent vehicle. This analysis, based on the assumption that plume merging takes place upstream of the dominant noise-producing region, may help simplify SLS and other rocket noise source modeling in the future.

Acknowledgments

The measurements were supported by the Utah NASA Space Grant Consortium, the BYU College of Physical and Mathematical Sciences, and Rollins College Hugh and Jeannette McKean Faculty Research Grant. Analysis was supported in part by National Science Foundation (NSF) Research Experiences for Undergraduates (REU) Grant No. 2051129 and NSF Grant No. 2109932.

References

[1] Gee, K. L., McLaughlin, B. W., Mathews, L.T., Edgington-Mitchell, D., Hart, G.W., and Anderson, M.C., "Launch Vehicle Noise and Australian Spaceports," *Proceedings of Meetings on Acoustics*, Vol. 52, No. 1, 2023, Paper 040002. https://doi.org/10.1121/2.0001856

[2] Gee, K. L., Lubert, C.P., and James, M.M., "The roar of a rocket," *Physics Today*, Vol. 77, No. 3, 2024, pp. 46–47. https://doi.org/10.1063/pt.izel.cyox

[3] Jones, N., "Does the roar of rocket launches harm wildlife? These scientists seek answers," *Nature*, Vol. 618, 2023, pp. 16–17. https://doi.org/10.1038/d41586-023-01713-7

[4] Henderson, B., Gerhart, C., Jensen, E., Griffin, S., and Lazzaro, A., "Vibro-acoustic launch protection experiment (VALPE)," *Journal of the Acoustical Society of America*, Vol. 114, No. 4, 2003, p. 2384. https://doi.org/10.1121/1.4809177

[5] Griffin, S., Lane, S., and Leo, D., "Innovative vibroacoustic control approaches in space launch vehicles," *Proceedings of INTER-NOISE 2000*, pp. 3583–3590. https://www.ingentaconnect.com/content/ince/incecp/2000/00002000/00000004/art00033

[6] Cole, J. N., Von Gierke, H. E., Kyrazis, D. T., Eldred, K. M., and Humphrey, A. J., "Noise radiation from fourteen types of rockets in the 1,000 to 130,000 pounds thrust range," Wright Air Development Center Technical Report 57-354, AD 130794, 1957.

[7] Guest, S. H., and Jones, J. H., "Far-field acoustic environmental predictions for launch of Saturn V and Saturn V MLV Configuration," NASA TN D-4117, Washington, DC, 1967.

[8] Wilhold, G. A., Guest, S. H., and Jones, J. H., "A technique for predicting far-field acoustic environments due to a moving rocket sound source," NASA TN D-1832, Washington, DC, 1963.
[9] Eldred, K. M., "Acoustic loads generated by the propulsion system," NASA SP-8072, 1971.
[10] McInerny, S. A., "Rocket noise-A review," AIAA Paper 90-3981, 1990. https://doi.org/10.2514/6.1990-3981
[11] McInerny, S. A., "Characteristics and predictions of far-field rocket noise," *Noise Control Engineering Journal*, Vol. 38, No. 1, 1992, pp. 5–16. https://doi.org/10.3397/1.2827802
[12] Sutherland, L. C., "Progress and problems in rocket noise prediction for ground facilities," AIAA Paper 93-4383, 1993. https://doi.org/10.2514/6.1993-4383
[13] Lubert, C. P., Gee, K. L., and Tsutsumi, S., "Supersonic jet noise from launch vehicles: 50 years since NASA SP-8072," *Journal of the Acoustical Society of America*, Vol. 151, No. 2, 2022, pp. 752–791. https://doi.org/10.1121/10.0009160
[14] Hart, G. W., Mathews, L. T., Anderson, M. C., Durrant, J. T., Bassett, M. S., Olausson, S. A., Houston, G., and Gee, K. L., "Methods and results of acoustical measurements made of a Delta IV Heavy launch," *Proceedings of Meetings on Acoustics*, Vol. 45, No. 1, 2022, Paper 040003. https://doi.org/10.1121/2.0001580
[15] Cunningham, C., Anderson, M. C., Moats, L. T., Gee, K. L., Hart, G. W., and Hall, L. K., "Acoustical measurement and analysis of an Atlas V launch," *Proceedings of Meetings on Acoustics*, Vol. 46, No.1, 2022, Paper 045005. https://doi.org/10.1121/2.0001742
[16] Gee, K. L., Mathews, L. T., Anderson, M. C., and Hart, G. W., "Saturn-V sound levels: A letter to the Redditor," *Journal of the Acoustical Society of America*, Vol. 152, No. 2, 2022, pp. 1068–1073. https://doi.org/10.1121/10.0013216
[17] Mathews, L. T., Gee, K. L., and Hart, G. W., "Characterization of Falcon 9 launch vehicle noise from far-field measurements," *Journal of the Acoustical Society of America*, Vol. 150, No. 1, 2021, pp. 620–633. https://doi.org/10.1121/10.0005658
[18] McInerny, S. A., "Launch vehicle acoustics Part 1: Overall levels and spectral characteristics," *Journal of Aircraft*, Vol. 33, No. 3, 1996, pp. 51–517. https://doi.org/10.2514/3.46974
[19] McInerny, S. A., "Launch vehicle acoustics Part 2: Statistics of the time domain data," *Journal of Aircraft*, Vol. 33, No. 3, 1996, pp. 518–523. https://doi.org/10.2514/3.46975
[20] McInerny, S. A., Wickiser, J. K., and Mellen, R. H., "Rocket noise propagation," *American Society of Mechanical Engineers Noise Control and Acoustics Division*, No. 24, 1997, pp. 37–50. https://doi.org/10.1115/IMECE1997-1027
[21] McInerny, S. A. and Ölçmen, S. M., "High-intensity rocket noise: Nonlinear propagation, atmospheric absorption, and characterization," *Journal of the Acoustical Society of America*, Vol. 117, No. 2, 2005, pp. 578–591. https://doi.org/10.1121/1.1841711
[22] Kandula, M., "Nearfield acoustics of clustered rocket engines," *Journal of Sound and Vibration*, Vol. 309, No. 3–5, 2008, pp. 852–857. https://doi.org/10.1016/j.jsv.2007.06.078
[23] Potter, R. C., and Crocker, M. J., "Acoustic prediction methods for rocket engines, including the effects of clustered engines and deflected exhaust flow," NASA-CR-566, Washington, DC, 1966.
[24] Northrop Grumman Innovation Systems, "Propulsion Products Catalog," Archived URL: https://web.archive.org/web/20190207020142/http://www.northropgrumman.com/Capabilities/PropulsionSystems/Documents/NGIS_MotorCatalog.pdf [cited 24 April 2024]. Sea level specific impulse calculated from specified vacuum conditions assuming a nominal 8% reduction at sea level relative to vacuum.
[25] L3Harris Technologies/Aerojet Rocketdyne, "RS-25 Engine," URL: https://www.l3harris.com/all-capabilities/rs-25-engine [cited 24 April 2024].
[26] James, M. M., Salton, A. R., Gee, K. L., Neilsen, T. B., McInerny, S. A., and Kenny, R. J., "Modification of directivity curves for a rocket noise model," *Proceedings of Meetings on Acoustics*, Vol. 18, No. 1, 2014, Paper 040008. https://doi.org/10.1121/1.4870986
[27] NASA, "NASA's Space Launch System Reference Guide (Version 2)," URL: https://www3.nasa.gov/sites/default/files/atoms/files/sls_reference_guide_2022_v2_508_0.pdf [cited 24 April 2024].
[28] L3Harris Technologies/Aerojet Rocketdyne, "RS-25 Propulsion System," URL: https://www.l3harris.com/resources/rs-25-propulsion-system-data-sheet [cited 24 April 2024].
[29] Northrop Grumman, "Propulsion Products Catalog," URL: https://www.northropgrumman.com/wp-content/uploads/NG-Propulsion-Products-Catalog.pdf [cited 24 April 2024].
[30] Rocketdyne Propulsion & Power, "Space Shuttle Main Engine Orientation," June 1998, URL: http://large.stanford.edu/courses/2011/ph240/nguyen1/docs/SSME_PRESENTATION.pdf [cited 24 April 2024].

[31] Gee, K. L., Hart, G. W., Cunningham, C. F., Anderson, M. C., Bassett, M. S., Mathews, L. T., Durrant, J. T., Moats, L. T., Coyle, W. L., Kellison, M. S., and Kuffskie, M. J., "Space Launch System acoustics: Far-field noise measurements of the Artemis-I launch," *JASA Express Letters*, Vol. 3, No. 2, 2023, Paper 023601. https://doi.org/10.1121/10.0016878

[32] Kellison, M. S. and Gee K. L., "Sound Power of NASA's lunar rockets: Space Launch System versus Saturn V," *JASA Express Letters*, Vol. 3, No. 11, 2023, Paper 113601. https://doi.org/10.1121/10.0022538

[33] Gee, K. L., Whiting, E. B., Neilsen, T. B., James, M. M., and Salton, A. R., "Development of a near-field intensity measurement capability for static rocket firings," *Transactions of the Japan Society for Aeronautical and Space Sciences, Aerospace Technology Japan*, Vol. 14, No. istis30, 2016, pp. Po_2_9–Po_2_15. https://doi.org/10.2322/tastj.14.Po_2_9

[34] Kellison, M. S., Gee, K. L., Cunningham, C. F., Coyle, W. L., Moore, T. M., and Hart, G. W., "Community-based noise measurements of the Artemis-I mission," *Proceedings of Meetings on Acoustics*, Vol. 51, No. 1, 2023, Paper 040004. https://doi.org/10.1121/2.0001786

[35] Gee, K. L., Novakovich, D. J., Mathews, L. T., Anderson, M. C., and Rasband, R. D., "Development of a Weather-Robust Ground-Based System for Sonic Boom Measurements," NASA/CR-2020-5001870, 2020. https://ntrs.nasa.gov/citations/20205001870

[36] GRAS, "GRAS 46BE Microphone Specifications," URL: https://www.grasacoustics.com/products/measurement-microphone-sets/constant-current-power-ccp/product/143-46be [cited 29 April 2024] .

[37] Marston, T. M., "Diffraction correction and low-frequency response extension for condenser microphones," M.S. Thesis, Graduate Program in Acoustics, Penn. State Univ., 2008.

[38] Rasband, R. D., Gee, K. L., Gabrielson, T. B., and Loubeau, A., "Improving low-frequency response of sonic boom measurements through digital filtering," *JASA Express Letters*, Vol. 3, No. 1, 2023, Paper 014802. https://doi.org/10.1121/10.0016751

[39] Anderson, M. C., Gee, K. L., Novakovich, D. J., Mathews, L. T., and Jones, Z. T., "Comparing two weather robust microphone configurations for outdoor measurements," *Proceedings of Meetings on Acoustics*, Vol. 42, No. 1, 2022, Paper 040005. https://doi.org/10.1121/2.0001561

[40] Gurbatov, S. N. and Rudenko, O. V, "Statistical phenomena," Chap. 13 in *Nonlinear Acoustics*, edited by M. F. Hamilton and D. T. Blackstock (Academic, San Diego, 1998), pp. 377–398.

[41] Bassett, M. S., Gee, K. L., Hart, G. W., Mathews, L. T., Rasband, R. D., and Novakovich, D. J., "Peak directivity analysis of far-field acoustical measurements during three GEM 63 static firings," *Proceedings of Meetings on Acoustics*, Vol. 39, No. 1, 2021, Paper 040004. https://doi.org/10.1121/2.0001467

[42] Kenny, R. J., Hobbs, C., Plotkin, K. J., and Pilkey, D., "Measurement and characterization of Space Shuttle solid rocket motor plume acoustics," AIAA Paper 2009-3161, 2009. https://doi.org/10.2514/6.2009-3161

[43] Fukuda, K., Fujii, K., Ui, K., Ishii, T., Oinuma, H., Kazawa, J., and Minesugi, K., "Acoustic measurements and prediction of solid rockets in static firing tests," AIAA Paper 2009-3368, 2009. https://doi.org/10.2514/6.2009-3368

[44] Christian, M. A., Gee, K. L., Streeter, J. B., Wall, A. T., and Campbell, S. C., "Sound power and acoustic efficiency of an installed GE F404 jet engine," *JASA Express Letters*, Vol. 3, No. 7, 2023, Paper 073601. https://doi.org/10.1121/10.0019866

[45] Mayes, W. H., Lanford, W. E., and Hubbard, H. H., "Near-field and far-field noise surveys of solid-fuel rocket engines for a range of nozzle exit pressures," NASA Report No. TN D-21, 1959. https://ntrs.nasa.gov/citations/19890068228

[46] Campos, E., "Prediction of noise from rocket engines," AIAA Paper 2005-2837, 2005. https://doi.org/10.2514/6.2005-2837

[47] James, M. M., Salton, A. R., Gee, K. L., Neilsen, T. B., and McInerny, S. A., "Full-scale rocket motor acoustic tests and comparisons with empirical source models," *Proceedings of Meetings on Acoustics*, Vol. 18, No. 1, 2014, Paper 040007. https://doi.org/10.1121/1.4870984

[48] Hart, G. W. and Gee, K. L., "Correcting for ground reflections when measuring overall sound power level and acoustic radiation efficiency of rocket launches," *Proceedings of Meetings on Acoustics*, Vol. 50, No. 1, 2023, Paper 040004. https://doi.org/10.1121/2.0001733

[49] Haynes, J. and Kenny, R. J., "Modifications to the NASA SP-8072 Distributed Source Method II for Ares I Lift-off Environment Predictions," AIAA Paper 2009-3160, 2009. https://doi.org/10.2514/6.2009-3160

[50] Hart, G. W., Gee, K. L., and Cook, M. R., "Corrected frequency-dependent directivity indices for large solid rocket motors," *Proceedings of Meetings on Acoustics*, Vol. 51, No. 1, 2023, Paper 040007. https://doi.org/10.1121/2.0001810

[51] Tam, C. K. W, "Mach wave radiation from high-speed jets," *AIAA Journal*, Vol. 47, No. 10, 2009, pp. 2440–2448. https://doi.org/10.2514/1.42644
[52] Seiner, J. M., Ponton, M. K., Jansen, B. J., and Lagen, N. T., "The effects of temperature on supersonic jet noise emission," AIAA Paper 92-2046, 1992.
[53] Greska, B., Krothapalli, A., Horne, W. C., and Burnside, N., "A Near-Field Study of High Temperature Supersonic Jets," AIAA Paper 2008-3026, 2008. https://doi.org/10.2514/6.2008-3026
[54] Oertel, H., "Measured Velocity Fluctuations Inside the Mixing Layer of a Supersonic Jet," in *Recent Contributions to Fluid Mechanics*, edited by W. Hasse (Springer-Verlag Berlin, Heidelberg), 1982, pp. 170-179. https://doi.org/10.1007/978-3-642-81932-2
[55] Mathews, L. T., Anderson, M. C., Gardner, C. D., McLaughlin, B. W., Hinds, B. M., McCullah-Boozer, M. R., Hall, L. K., and Gee K. L., "An overview of acoustical measurements made of the Atlas V JPSS-2 rocket launch," *Proceedings of Meetings on Acoustics*, Vol. 51, No. 1, 2023, Paper 040003. https://doi.org/10.1121/2.0001768